

# Four new Ni<sup>II</sup> antiferromagnetic complexes with azido bridges

Montserrat Monfort,<sup>\*a</sup> Inmaculada Resino,<sup>a</sup> Joan Ribas,<sup>a</sup> Xavier Solans,<sup>b</sup> Mercé Font-Bardia<sup>b</sup> and Helen Stoeckli-Evans<sup>c</sup>

<sup>a</sup> Departament de Química Inorgànica, Universitat de Barcelona, Martí i Franqués 1-11, 08028, Barcelona, Spain. E-mail: montserrat.monfort@qi.ub.es.; Fax: (34) 93 490 77 25

<sup>b</sup> Departament de Cristal·lografia i Mineralogia, Universitat de Barcelona, Martí i Franqués s/n, 08028, Barcelona, Spain

<sup>c</sup> Institute de Chimie, Université de Neuchâtel, Av. De Bellevaux 51, 2000, Neuchâtel, Switzerland

Received (in London, UK) 4th June 2002, Accepted 24th September 2002

First published as an Advance Article on the web 10th October 2002

Four new nickel(II) compound with formulas *trans-catena*-[Ni(*N*-Pren)<sub>2</sub>(μ<sub>1,3</sub>-N<sub>3</sub>)](ClO<sub>4</sub>) (1), *trans-catena*-[Ni(*N,N*-Me<sub>2</sub>en)<sub>2</sub>(μ<sub>1,3</sub>-N<sub>3</sub>)](PF<sub>6</sub>) (2), *trans-catena*-[Ni(*N,N'*-Pren)<sub>2</sub>(μ<sub>1,3</sub>-N<sub>3</sub>)](PF<sub>6</sub>) (3) and [Ni(*N*-Metn)<sub>2</sub>(μ<sub>1,3</sub>-N<sub>3</sub>)]<sub>2</sub>(ClO<sub>4</sub>)<sub>2</sub> (4) (*N*-Pren = *N*-propylethylenediamine, *N,N*-Me<sub>2</sub>en = *N,N*-dimethylethylenediamine, *N,N'*-Pren = *N,N'*-dipropylethylenediamine and *N*-Metn = *N*-methylpropanediamine) were synthesized and characterised. A single-crystal structure analysis revealed that compounds (1), (2) and (3) consist of a single end-to-end azido bridged nickel(II) chains in *trans* position, whereas compound (4) is a dinuclear Ni<sup>II</sup> complex with double end-to-end azido bridges between the two nickel(II) centres. From the magnetic point of view, compounds (1) and (2) are uniform antiferromagnetic one-dimensional chains with only one value of *J* and *g*. Compound (3) shows two kinds of Ni<sup>II</sup> in the structure, but all the azido bridges are equivalent, which generates only one value for the superexchange *J* but two values for *g*. Compound (4) shows moderate antiferromagnetic coupling. The best fit parameters obtained for all the compounds are in agreement with the structural parameters and compares well with other similar compounds reported in the literature.

## Introduction

Exchange interactions propagated by multi-atom bridges between paramagnetic centres have attracted great interest in the past few years. The azide bridge can generate systems ranging from discrete molecules with different nuclearity to 3-D compounds.<sup>1</sup> Focusing our attention on 1-D nickel-azide systems, the versatility of the bridging ligand generates a large number of topologies: homogenous or alternating chains with a single end-to-end (EE) bridge in *trans* or *cis* arrangement, uniform chains with a double end-to-end bridge, or alternating chains with end-to-end and end-on (EO) bridges in different distributions.<sup>1</sup> One dimensional compounds with a single EE azido bridge usually show antiferromagnetic coupling. To our knowledge only two 1-D azido-bridged Ni(II) compounds<sup>2,3</sup> show ferromagnetic coupling, in which the torsion angle for the azido bridge is 75.7° and 106.8° respectively, in the range where the antiferromagnetic contribution is minimised to favour the ferromagnetic contribution.<sup>4</sup> On the other hand, all the dinuclear compounds with a double EE azido bridge reported so far are antiferromagnetically coupled.

Using bidentate compounds as ancillary ligands in a metal-ligand ratio of 1:2 there are two free positions in the coordination sphere of Ni<sup>II</sup> that should be completed by an azido ligand in the *cis* or *trans* position, giving a one-dimensional or a dinuclear cationic compound. In this study, using different *N*-substituted derivatives of ethylenediamine as ancillary bidentate ligands, we report the synthesis, structure and magnetic properties of three new one-dimensional compounds: *trans*-[Ni(*N*-Pren)<sub>2</sub>(μ<sub>1,3</sub>-N<sub>3</sub>)]<sub>n</sub>(ClO<sub>4</sub>)<sub>n</sub> (1), *trans*-[Ni(*N,N*-Me<sub>2</sub>en)<sub>2</sub>(μ<sub>1,3</sub>-N<sub>3</sub>)]<sub>n</sub>(PF<sub>6</sub>)<sub>n</sub> (2) and *trans*-[Ni(*N,N'*-Pren)<sub>2</sub>(μ<sub>1,3</sub>-N<sub>3</sub>)]<sub>n</sub>(PF<sub>6</sub>)<sub>n</sub> (3). Compounds (1) and (2) are uniform chains with only one kind of Ni<sup>II</sup> and all the azido bridges are equivalent,

giving uniform antiferromagnetic chains. Compound (3) has two different Ni<sup>II</sup> ions located in an inversion centre; all the azido bridges are equivalent, which gives a structurally uniform antiferromagnetic chain with only one value of the superexchange coupling *J* and two different values of *g*. When we use *N*-Metn as a bidentate amine, two positions remain free around the Ni<sup>II</sup> coordination sphere, giving in this case a dinuclear [Ni(*N*-Metn)<sub>2</sub>(μ<sub>1,3</sub>-N<sub>3</sub>)]<sub>2</sub>(ClO<sub>4</sub>)<sub>2</sub> (4) compound.

## Experimental

### General remarks

All operations were carried out in an open atmosphere and at room temperature. All reagents were purchased from Aldrich Company and used as supplied. Magnetic measurements were carried out on polycrystalline samples with a pendulum type magnetometer (MANICS DSM8) equipped with a helium continuous-flow cryostat, working in the temperature range 4–300 K, and a Bruker BE15 electromagnet. The magnetic field was 15000 G. Diamagnetic corrections were estimated from Pascal tables.

### Synthesis

*trans*-[Ni(*N*-Pren)<sub>2</sub>(μ<sub>1,3</sub>-N<sub>3</sub>)]<sub>n</sub>(ClO<sub>4</sub>)<sub>n</sub> (1). *N*-Pren (0.41 g, 4 mmol) was added to a solution of Ni(ClO<sub>4</sub>)<sub>2</sub>·6H<sub>2</sub>O (0.73 g, 2 mmol) in dimethylformamide:ethanol (2:1, 30 ml), followed by the slow addition with continuous stirring of NaN<sub>3</sub> (0.13 g, 2 mmol) in the solid state. After being stirred for 15 minutes the clear green blue solution was filtered to remove any impurities and left to stand undisturbed at room temperature. Single blue crystals of (1) were collected after two months;

the yield was approximately 65%. (Found C, 29.7; H, 7.0; N, 24.2%.  $C_{10}H_{28}ClN_7NiO_4$  requires C, 29.8; H, 7.0; N, 24.3%.)

***trans*-[Ni(*N,N*-Me<sub>2</sub>en)<sub>2</sub>(μ<sub>1,3</sub>-N<sub>3</sub>)<sub>*n*</sub>](PF<sub>6</sub>)<sub>*n*</sub> (2).** (0.13 g, 2 mmol) of NaN<sub>3</sub> in the solid state was added slowly to a solution of Ni(NO<sub>3</sub>)<sub>2</sub>·6H<sub>2</sub>O (0.58 g, 2 mmol) and *N,N*-Me<sub>2</sub>en (0.35 g, 4 mmol) in acetonitrile/water (1:3, 30 ml). After filtration to remove any impurities, (0.40 g, 2.5 mmol) of NH<sub>4</sub>PF<sub>6</sub> dissolved in water (3 ml) was added with continuous stirring. The solution was left undisturbed, and rectangular blue crystals of (2) were obtained after several days; the yield was approximately 75%. (Found C, 22.8; H, 5.7; N, 23.0%.  $C_8H_{20}F_6N_7NiP$  requires C, 22.8; H, 5.7; N, 23.3%.)

***trans*-[Ni(*N,N'*-Pr<sub>2</sub>en)<sub>2</sub>(μ<sub>1,3</sub>-N<sub>3</sub>)<sub>*n*</sub>](PF<sub>6</sub>)<sub>*n*</sub> (3).** Complex (3) was prepared in the same way as compound (2) but using *N,N'*-Pr<sub>2</sub>en (0.58 g, 4 mmol) instead of *N,N*-Me<sub>2</sub>en. The resulting blue mixture was left to evaporate. After a few days fine, pale blue crystals were obtained; the yield was approximately 70%. (Found C 35.8; H 7.8, N 18.3%.  $C_8H_{20}F_6N_7NiP$  requires C, 36.0; H, 7.6; N, 18.4%.)

***trans*-[Ni(*N*,Metn)<sub>2</sub>(μ<sub>1,3</sub>-N<sub>3</sub>)<sub>*n*</sub>](ClO<sub>4</sub>)<sub>*n*</sub> (4).** Complex (4) was prepared in the same way as compound (1) but using *N*-Metn (0.35 g, 4 mmol) instead of *N*-Pren. The resulting blue solution was sealed in a recipient with ether atmosphere as precipitant. Blue crystals suitable for X-ray determination were obtained after several days; the yield was approximately 75%. (Found C, 25.7; H, 6.4; N, 25.8%.  $C_{16}H_{48}Cl_2N_{14}Ni_2O_8$  requires C, 25.6; H, 6.4; N, 26.1%.)

**Caution!** Perchlorate salts of compounds containing organic ligands and azido complexes of metal ions are potentially explosive. Only small quantities of these compounds should be prepared and they should be handled behind suitable protective shields.

## Crystal data collection and refinement

Data collection for (2), (3) and (4) was performed with an Enraf Nonius Cad4 diffractometer with graphite-monochromated Mo-K<sub>α</sub> radiation ( $\lambda = 0.71069$  Å) at room temperature. Intensities were collected by the  $\omega$ -2 $\theta$  scan technique. Intensity data for (1) were collected on a Stoe Image Plate Diffraction System also using graphite-monochromated Mo-K<sub>α</sub> radiation ( $\lambda = 0.71073$  Å). Exposure time was 240 s per frame collected using the  $\phi$ -scan technique. The reflections collected in the four structures were corrected for Lorentz and polarization effects.

All structures were solved by direct methods using SHELXS<sup>5</sup> (1993 version for (2) and (3), and 1997 version for (1) and (4)) and refined by the full-matrix least-square method on  $F^2$  using SHELXL.<sup>6</sup> In (3), the fluorine atoms of PF<sub>6</sub><sup>−</sup> and C(5) were located in disordered sites. The occupancy factor of C(5) was refined giving a value of 0.61(2) for C(5) and 0.39(2) for C(5') sites, while the fluorine atoms were refined using an occupancy factor of 0.5 according to the height of Fourier synthesis. C(4) and C(5) atoms of (1) were also located in disordered sites. The occupancy factor of C(4A) and C(5A) was 0.564(18), while it was 0.436(18) for C(4B) and C(5B). All hydrogen atoms of (4) were located from a difference Fourier synthesis and refined isotropically, while the hydrogen atoms of the remaining structures were placed at calculated positions riding on the parent carbon atoms. The isotropic temperature factor was 1.2 times the equivalent temperature factor of the linked carbon atom. Details of data collection and refinement are shown in Table 1.

CCDC reference numbers 186790–186793. See <http://www.rsc.org/suppdata/nj/b2/b205404c/> for crystallographic data in CIF or other electronic format.

## Description of the structures

***trans*-[Ni(*N*-Pren)<sub>2</sub>(μ<sub>1,3</sub>-N<sub>3</sub>)<sub>*n*</sub>](ClO<sub>4</sub>)<sub>*n*</sub> (1).** The structure consists of cationic chains of nickel atoms linked by EE azido bridges, isolated by ClO<sub>4</sub><sup>−</sup> anions in the interchain space.

**Table 1** Crystallographic data from the X-ray diffraction studies of (1), (2), (3) and (4)

	(1)	(2)	(3)	(4)
Empirical formula	C <sub>10</sub> H <sub>28</sub> ClN <sub>7</sub> NiO <sub>4</sub>	C <sub>8</sub> H <sub>24</sub> F <sub>6</sub> N <sub>7</sub> NiP	C <sub>16</sub> H <sub>32</sub> F <sub>6</sub> N <sub>7</sub> NiP	C <sub>8</sub> H <sub>24</sub> ClN <sub>7</sub> NiO <sub>4</sub>
Formula weight	404.61	422.02	526.17	376.50
Temperature/K	293 (2)	293 (2)	293 (2)	293 (2)
$\lambda$ (Mo-K $\alpha$ )/Å	0.71073	0.71069	0.71069	0.71069
Crystal system	Monoclinic	Triclinic	Monoclinic	Monoclinic
Space group	<i>P</i> 2	<i>P</i> 1̄	<i>P</i> 2 <sub>1</sub> / <i>n</i>	<i>P</i> 2 <sub>1</sub> / <i>n</i>
<i>a</i> /Å	8.3715(7)	6.39(2)	11.258(3)	10.401(2)
<i>b</i> /Å	18.4000(12)	8.84(4)	12.380(10)	9.286(3)
<i>c</i> /Å	12.2042(9)	9.102(7)	18.941(5)	17.429(2)
$\alpha$ /°	90	116.8(2)	90	90
$\beta$ /°	95.958(10)	91.9(2)	103.43(2)	106.8(6)
$\gamma$ /°	90	109.1 (3)	90	90
<i>V</i> /Å <sup>3</sup>	1869.7(2)	424(2)	2568(2)	1614.8(6)
<i>Z</i>	4	1	4	4
$\rho_{\text{calcd.}}$ /Mg cm <sup>−3</sup>	1.437	1.654	1.361	1.549
$\mu$ /mm <sup>−1</sup>	1.141	1.306	0.877	1.396
<i>F</i> (000)	856	218	1096	792
Scan range $\theta$ /°	2.45–25.97	2.56–29.96	1.93–29.98	2.06–29.98
Index ranges ( <i>h,k,l</i> )	−10/10, −22/22, −14/14	−8/8, −12/11, 0/12	−15/15, −2/17, −7/24	−14/14, 0/13, −3/24
Reflections collected	14 522	1789	7161	4836
Independent reflections	3628	1770	6879	4690
Observed ( <i>I</i> > 2 $\sigma$ ( <i>I</i> ))	1986	1566	2297	2780
<i>R</i> (int)	0.057	0.032	0.016	0.046
Data/parameters	3628/231	1720/111	4819/372	4640/287
Goodness-of-fit	0.801	0.984	1.006	0.998
Final <i>R</i> indices <i>I</i> > 2 $\sigma$ ( <i>I</i> )	<i>R</i> = 0.038	<i>R</i> = 0.054	<i>R</i> = 0.061	<i>R</i> = 0.054
	$\omega R_2$ = 0.082	$\omega R_2$ = 0.126	$\omega R_2$ = 0.147	$\omega R_2$ = 0.116
$\Delta\rho$ max/min/e Å <sup>−3</sup>	0.43/0.37		0.64/−0.41	0.57/−0.67

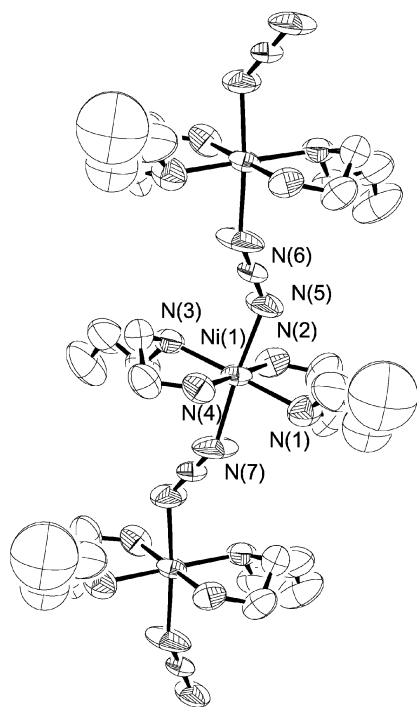


**Fig. 1** ORTEP drawing and labeling scheme of the cationic part of  $trans-[Ni(N-Pren)_2(\mu_{1,3}-N_3)]_n(ClO_4)_n$  (**1**). Ellipsoids at the 50% probability level.

The chain runs along the (0 0 1) direction. In the chain structure each Ni(II) atom is coordinated by two bidentate *N-Pren* ligands and two azido ligands in a distorted octahedral *trans* arrangement. A labeled scheme of the cationic part is shown in Fig. 1. The four N atoms of the diamine ligands and the Ni<sup>II</sup> atom are in the same plane (maximum deviation from plane: 0.012 Å for N(1)). The four Ni–N<sub>amine</sub> distances are different, the two longest distances correspond to two Ni–N<sub>amine</sub> coordinated to propyl ligands (2.124(4) and 2.119(3) Å) in *trans* positions, creating a rhomboidal distortion. All the Ni<sup>II</sup> are equivalent but the coordination of the azido bridge is asymmetrical; the two Ni–N<sub>azido</sub> distances are 2.113(3) Å (Ni–N<sub>5</sub>) and 2.121(3) Å (Ni–N<sub>7</sub>) and the Ni–N–N angles are 136.4(3)° (Ni–N(5)–N(6)) and 149.8(3)° (Ni–N(7)–N(6)). This produces a uniform –Ni–N<sub>a</sub>–N<sub>b</sub>–N<sub>c</sub>–Ni–N<sub>a</sub>–N<sub>b</sub>–N<sub>c</sub>–Ni– chain. The Ni–N<sub>3</sub>–Ni torsion angle is 161.2°. The main bond lengths and angles are listed in Table 2.

**Table 2** Selected bond lengths [Å] and angles [°] for:  $trans-[Ni(N-Pren)_2(\mu_{1,3}-N_3)]_n(ClO_4)_n$  (**1**)

Ni(1)–N(4)	2.088(3)	Ni(1)–N(7)	2.121(3)
Ni(1)–N(2)	2.090(3)	Ni(1)–N(1)	2.124(4)
Ni(1)–N(5)	2.113(3)	N(5)–N(6)	1.141(4)
Ni(1)–N(3)	2.119(3)		
N(6)–N(7)#1	1.126(4)		
N(4)–Ni(1)–N(2)	179.39(14)	N(3)–Ni(1)–N(7)	95.00(13)
N(4)–Ni(1)–N(5)	94.28(13)	N(4)–Ni(1)–N(1)	96.87(14)
N(2)–Ni(1)–N(5)	85.77(13)	N(2)–Ni(1)–N(1)	83.73(14)
N(4)–Ni(1)–N(3)	83.55(13)	N(5)–Ni(1)–N(1)	91.48(15)
N(2)–Ni(1)–N(3)	95.84(13)	N(3)–Ni(1)–N(1)	178.81(12)
N(5)–Ni(1)–N(3)	89.60(14)	N(7)–Ni(1)–N(1)	83.91(14)
N(4)–Ni(1)–N(7)	88.13(15)	N(6)–N(5)–Ni(1)	136.4(3)
N(2)–Ni(1)–N(7)	91.87(16)	N(7)#1–N(6)–N(5)	179.6(4)
N(5)–Ni(1)–N(7)	175.03(17)	N(6)#2–N(7)–Ni(1)	149.8(3)

Symmetry transformation used to generate equivalent atoms: #1 = *x*, –*y* + 1/2, *z* – 1/2 #2 = *x*, –*y* + 1/2, *z* + 1/2.

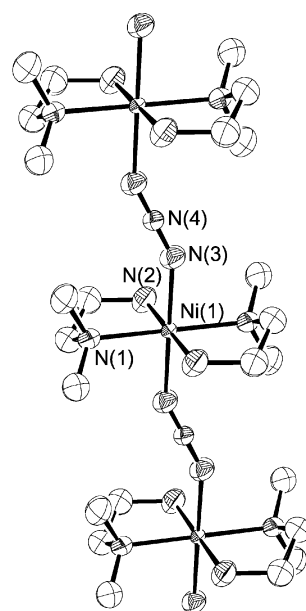


**Fig. 2** ORTEP drawing of  $trans-[Ni(N,N-Me_2en)_2(\mu_{1,3}-N_3)]_n(PF_6)_n$  (**2**), which shows atom labeling scheme of the cationic part. Ellipsoids at the 50% probability level.

$trans-[Ni(N,N-Me_2en)_2(\mu_{1,3}-N_3)]_n(PF_6)_n$  (**2**). This structure consists of cationic chains of Ni(II) atoms linked by EE azido bridges, isolated by PF<sub>6</sub><sup>–</sup> anions in the interchain space. The chain runs along the [0 0 1] direction. An ORTEP plot of the cationic part is shown in Fig. 2. The main bond lengths and angles are gathered in Table 3. All the Ni<sup>II</sup> are equivalently located on the inversion centre and related by an inversion centre situated in the central nitrogen atom of the azido ligand. This produces a uniform –Ni–N<sub>a</sub>–N<sub>b</sub>–N<sub>c</sub>–Ni–N<sub>a</sub>–N<sub>b</sub>–N<sub>c</sub>–Ni– chain. Each Ni<sup>II</sup> is surrounded by six nitrogen atoms; four belong to two diamines in *trans* positions, and two belong to N<sub>3</sub><sup>–</sup> bridging ligands, also in *trans* position. The NiN<sub>6</sub> core is a slightly distorted octahedron. The four N atoms of the diamine ligands and the Ni<sup>II</sup> atom are in the same plane. All the N–Ni–N angles in *trans* positions are 180°. There are two different Ni–N<sub>amine</sub> distances: the longer of these always corresponds to the Ni–N<sub>amine</sub> coordinated to the *N,N*-Me<sub>2</sub> ligand (2.190(12) Å). The Ni–N<sub>azido</sub> distance is 2.122(8) Å and the Ni–azido angle is 151.4(4)°. The Ni–N<sub>3</sub>–Ni torsion angle is 180.0°.

**Table 3** Selected bond lengths [Å] and angles [°] for:  $trans-[Ni(N,N-Me_2en)_2(\mu_{1,3}-N_3)]_n(PF_6)_n$  (**2**)

Ni(1)–N(2)	2.087(5)	Ni(1)–N(1)#1	2.190(12)
Ni(1)–N(2)#1	2.087(5)	Ni(1)–N(1)	2.190(12)
Ni(1)–N(3)	2.122(8)	N(3)–N(4)	1.164(6)
Ni(1)–N(3)#1	2.122(8)	N(4)–N(3)#2	1.164(6)
N(2)–Ni(1)–N(2)#1	180.0	N(3)#1–Ni(1)–N(1)#1	93.3(4)
N(2)–Ni(1)–N(3)	90.0(2)	N(2)–Ni(1)–N(1)	83.8(3)
N(2)#1–Ni(1)–N(3)	90.0(2)	N(2)#1–Ni(1)–N(1)	96.2(3)
N(2)–Ni(1)–N(3)#1	90.0(2)	N(3)–Ni(1)–N(1)	93.3(4)
N(2)#1–Ni(1)–N(3)#1	90.0(2)	N(3)#1–Ni(1)–N(1)	86.7(4)
N(3)–Ni(1)–N(3)#1	180.0	N(1)#1–Ni(1)–N(1)	180.0
N(2)–Ni(1)–N(1)#1	96.2(3)	N(4)–N(3)–Ni(1)	151.4(4)
N(2)#1–Ni(1)–N(1)#1	83.8(3)	N(4)–N(3)#1–Ni(1)	151.4(4)
N(3)–Ni(1)–N(1)#1	86.7(4)	N(3)#2–N(4)–N(3)	180.0

Symmetry transformation used to generate equivalent atoms: #1 = –*x*, –*y*, –*z*, #2 = –*x* + 1, –*y*, –*z*, #3 = –*x* + 1, –*y*, –*z* + 1.

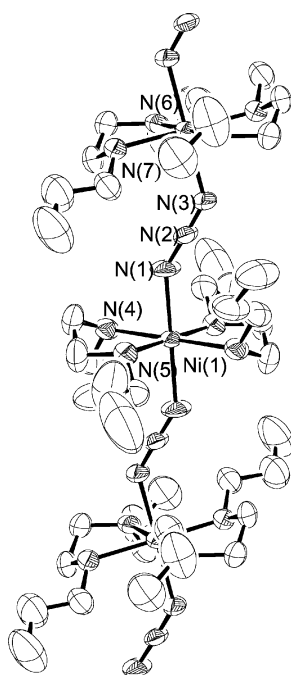


**Fig. 3** ORTEP drawing and labeling scheme of the cationic part of  $\text{trans-[Ni(N,N'-Pren)}_2(\mu_{1,3}\text{-N}_3)]_n(\text{PF}_6)_n$  (**3**). Ellipsoids at the 50% probability level.

**$\text{trans-[Ni(N,N'-Pren)}_2(\mu_{1,3}\text{-N}_3)]_n(\text{PF}_6)_n$  (**3**).** This structure also consists of cationic chains of nickel atoms linked by EE azido bridges, isolated by  $\text{PF}_6^-$  anions in the interchain space. The chain runs along the  $[0\ 1\ 0]$  direction. An ORTEP plot of the cationic part is shown in Fig. 3. The main bond lengths and angles are gathered in Table 4. There are two different  $\text{Ni}^{\text{II}}$  in the chain located on an inversion centre; this produces an alternating  $\text{-Ni-N}_a\text{-N}_b\text{-N}_c\text{-Ni-N}_c\text{-N}_b\text{-N}_a\text{-Ni-}$  chain with only one kind of azido bridge. Each  $\text{Ni}^{\text{II}}$  ion is octahedrally

**Table 4** Selected bond lengths [Å] and angles [°] for  $\text{trans-[Ni(N,N'-Pren)}_2(\mu_{1,3}\text{-N}_3)]_n(\text{PF}_6)_n$  (**3**)

Ni(1)–N(4)#1	2.108(5)	Ni(2)–N(3)	2.099(5)
Ni(1)–N(4)	2.108(5)	Ni(2)–N(6)#2	2.152(6)
Ni(1)–N(1)	2.123(5)	Ni(2)–N(6)	2.152(6)
Ni(1)–N(1)#1	2.123(5)	Ni(2)–N(7)#2	2.161(5)
Ni(1)–N(5)#1	2.144(5)	Ni(2)–N(7)	2.161(5)
Ni(1)–N(5)	2.144(5)	N(1)–N(2)	1.159(6)
Ni(2)–N(3)#2	2.099(5)	N(2)–N(3)	1.171(6)

N(4)#1–Ni(1)–N(4)	180.0	N(3)–Ni(2)–N(6)#2	88.7(2)
N(4)#1–Ni(1)–N(1)	93.2(2)	N(3)#2–Ni(2)–N(6)	88.7(2)
N(4)–Ni(1)–N(1)	86.8(2)	N(3)–Ni(2)–N(6)	91.3(2)
N(4)#1–Ni(1)–N(1)#1	86.8(2)	N(6)#2–Ni(2)–N(6)	180.0
N(4)–Ni(1)–N(1)#1	93.2(2)	N(3)#2–Ni(2)–N(7)#2	95.3(2)
N(1)–Ni(1)–N(1)#1	180.0	N(3)–Ni(2)–N(7)#2	84.7(2)
N(4)#1–Ni(1)–N(5)#1	83.0(2)	N(6)#2–Ni(2)–N(7)#2	82.4(2)
N(4)–Ni(1)–N(5)#1	97.0(2)	N(6)–Ni(2)–N(7)#2	97.6(2)
N(1)–Ni(1)–N(5)#1	91.8(2)	N(3)#2–Ni(2)–N(7)	84.7(2)
N(1)#1–Ni(1)–N(5)#1	88.2(2)	N(3)–Ni(2)–N(7)	95.3(2)
N(4)#1–Ni(1)–N(5)	97.0(2)	N(6)#2–Ni(2)–N(7)	97.6(2)
N(4)–Ni(1)–N(5)	83.0(2)	N(6)–Ni(2)–N(7)	82.4(2)
N(1)–Ni(1)–N(5)	88.2(2)	N(7)–Ni(2)–N(7)#	180.0
N(1)#1–Ni(1)–N(5)	91.8(2)	N(3)–Ni(2)–N(1)	178.5(5)
N(5)#1–Ni(1)–N(5)	180.0	N(2)–Ni(3)–Ni(2)	145.4(3)
N(3)#2–Ni(2)–N(3)	180.0	N(2)–Ni(1)–Ni(1)	136.5(4)
N(3)#2–Ni(2)–N(6)#2	91.3(2)		

Symmetry transformation used to generate equivalent atoms: #1 =  $-x, -y + 1, -z$ , #2 =  $-x, -y + 2, -z$ .

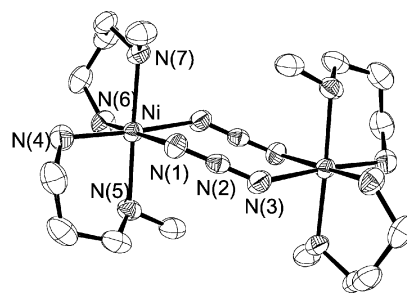


**Fig. 4** ORTEP drawing and labeling scheme of the cationic part of  $[\text{Ni(N-Metn)}_2(\mu_{1,3}\text{-N}_3)]_2(\text{ClO}_4)_2$  (**4**). Ellipsoids at the 50% probability level.

coordinated to two  $\text{N,N'-Pren}$  and two  $\text{N}_3^-$  bridging ligands in *trans* positions. The  $\text{NiN}_6$  core is a slightly distorted octahedron. The four N atoms of the diamine ligands and the  $\text{Ni}^{\text{II}}$  atom are in the same plane. All the N–Ni–N angles in *trans* positions are  $180^\circ$ . There are two different Ni– $\text{N}_{\text{amine}}$  distances for each different  $\text{Ni}^{\text{II}}$  ion. The Ni– $\text{N}_{\text{amine}}$  bond lengths range from 2.108(5) to 2.161(6) Å. The Ni– $\text{N}_{\text{azide}}$  distances are 2.123(5) Å for Ni(1) and 2.099(5) Å for Ni(2). The Ni–azido angles are Ni–N<sub>1</sub>–N<sub>2</sub> =  $136.5^\circ$  and Ni–N<sub>3</sub>–N<sub>2</sub> =  $145.4^\circ$ . The Ni–N<sub>3</sub>–Ni torsion angle is  $177.6^\circ$ .

**$[\text{Ni(N-Metn)}_2(\mu_{1,3}\text{-N}_3)]_2(\text{ClO}_4)_2$  (**4**).** The unit cell contains two dinuclear Ni–Ni cations and four  $\text{ClO}_4^-$  anions. Two of the dinuclear entities are placed in the  $(1\ 0\ 1)$  plane, and the others two ones are placed on  $(0\ 0\ 1)$  axes. The labeling scheme is shown in Fig. 4. The main bond lengths and angles are listed in Table 5. The nickel atom occupies a distorted octahedral environment, formed by two N atoms of the two azido bridging ligand and four N atoms of the two bidentate  $\text{N-Metn}$  amine. The two *cis* Ni– $\text{N}_{\text{azide}}$  distances are 2.131(3) and 2.202(3) Å. The Ni– $\text{N}_{\text{amine}}$  bond lengths range from 2.085(3) to 2.162(3) Å, the two shortest distances being the two Ni– $\text{N}_{\text{amine}}$  non-substituted bonds *trans* to the Ni– $\text{N}_{\text{azide}}$  bonds. The Ni– $\text{N}_{\text{azide}}$  angles are Ni–N<sub>1</sub>–N<sub>2</sub> =  $124.0(2)^\circ$  and Ni–N<sub>3</sub>–N<sub>2</sub> =  $134.7(2)^\circ$ , and the  $\text{N}_3\text{-Ni-N}_1$  angle is  $89.03(11)^\circ$ . The dihedral angle  $\delta$  (which is defined as the angle between the  $(\text{N}_3)_2$  (least-square) plane and the N–Ni–N plane) is  $24.8^\circ$ , giving a chairlike structure.

## Magnetic properties

The variable temperature magnetic susceptibility data were recorded for all compounds between 300–4 K. All the

**Table 5** Selected bond lengths [Å] and angles [°] for  $[\text{Ni(N-Metn)}_2(\mu_{1,3}\text{-N}_3)]_2(\text{ClO}_4)_2$  (**4**)

Ni–N(4)	2.085(3)	Ni–N(3)#1	2.202(3)
Ni–N(6)	2.092(3)	N(1)–N(2)	1.171(4)
Ni–N(1)	2.131(3)	N(2)–N(3)	1.166(4)
Ni–N(7)	2.139(3)	N(3)–Ni#1	2.202(3)
Ni–N(5)	2.162(3)		
N(4)–Ni–N(6)	93.17(15)	N(7)–Ni–N(5)	177.60(12)
N(4)–Ni–N(1)	93.92(13)	N(4)–Ni–N(3)#1	175.34(12)
N(6)–Ni–N(1)	172.34(13)	N(6)–Ni–N(3)#1	84.08(14)
N(4)–Ni–N(7)	93.25(14)	N(1)–Ni–N(3)#1	89.03(11)
N(6)–Ni–N(7)	93.63(13)	N(7)–Ni–N(3)#1	83.19(12)
N(1)–Ni–N(7)	88.85(11)	N(5)–Ni–N(3)#1	96.39(12)
N(4)–Ni–N(5)	87.29(14)	N(2)–N(1)–Ni	124.0(2)
N(6)–Ni–N(5)	88.68(13)	N(3)–N(2)–N(1)	177.9(3)
N(1)–Ni–N(5)	88.78(12)	N(2)–N(3)–Ni#1	134.7(2)

Symmetry transformations used to generate equivalent atoms: #1 =  $-x + 1, -y + 1, -z$ .

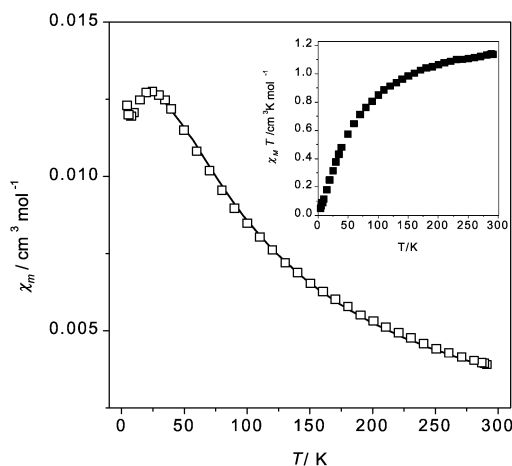


**Fig. 5** Plots of observed  $\chi_M$  and  $\chi_M T$  (inset) versus  $T$  for *trans*-[Ni(*N*-Pren) $_2(\mu_{1,3}$ -N $_3$ )] $_n$ (ClO $_4$ ) $_n$  (**1**). Solid line represents the best theoretical fit (see text).

compounds show an antiferromagnetic interaction between the metal ions. Magnetic data for compounds (**1**), (**2**), (**3**) and (**4**) are plotted in Figs. 5, 6, 7 and 8 respectively. In all cases, the molar susceptibility increases when the temperature decreases; it reaches a maximum (at 25 K for (**1**), at 7 K for (**2**), at 49 K for (**3**) and at 100 K for (**4**)) and below these temperatures the curve decreases continuously to 4 K (the increase in the susceptibility when the compound cools to very low temperature, for compound (**1**), may be due to the presence of monomeric Ni<sup>II</sup> ions in the polycrystalline powder sample).  $\chi_M T$  decreases continuously from room temperature and tends to zero at 4 K.

According to the structural data, compounds (**1**) and (**2**) are uniform  $S = 1$  one-dimensional systems with only one intramolecular coupling constant,  $J$ , and only one Landé factor  $g$ . For compound **3** the structural data reveal two kinds of Ni<sup>II</sup> ions and only one kind of azido bridge: this provides only one intramolecular coupling constant,  $J$ , and two different and alternating  $g$  values. Taking into account the very small differences between the two Ni<sup>II</sup> environments we interpret the experimental data on the basis of an average  $g$  value.

For systems of this kind, isotropic 1-D  $S = 1$ , the temperature dependence of the susceptibility extrapolated from calculations performed on ring systems of increasing length is given by Weng,<sup>7</sup> using the hamiltonian  $H = -J \sum S_i S_{i+1}$ . The Weng equation is valid only for antiferromagnetic coupling.

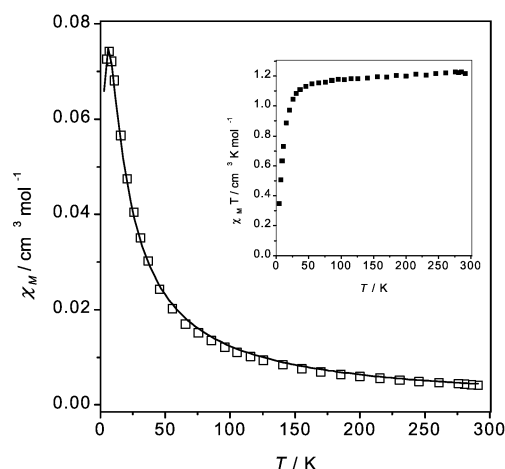


**Fig. 6** Plots of observed  $\chi_M$  and  $\chi_M T$  (inset) versus  $T$  for *trans*-[Ni(*N,N*-Me $_2$ en) $_2(\mu_{1,3}$ -N $_3$ )] $_n$ (PF $_6$ ) $_n$  (**2**). Solid line represents the best theoretical fit (see text).

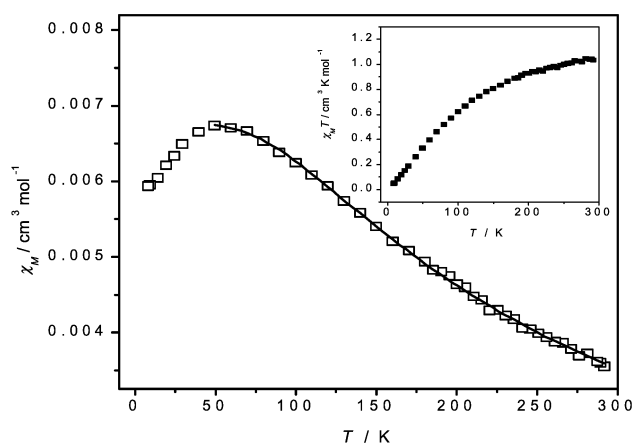


**Fig. 7** Plots of observed  $\chi_M$  and  $\chi_M T$  (inset) versus  $T$  for *trans*-[Ni(*N,N'*-Pren) $_2(\mu_{1,3}$ -N $_3$ )] $_n$ (PF $_6$ ) $_n$  (**3**). Solid line represents the best theoretical fit (see text).

A good fit is possible only down to a temperature near the maximum of  $\chi_M$  because neither zero-field splitting nor the Haldane gap effect<sup>8</sup> is taken into account. Using this equation, the theoretical result affords a satisfactory agreement with the experimental data points as illustrated in Figs. 5, 6, and 7 respectively. The best fitted parameters are gathered in Table 6.

Experimental data for (**4**) were analysed using the isotropic Heisenberg model with  $H = -JS_1S_2$ , assuming a negligible effect of zero field splitting at the temperature of maximum susceptibility.<sup>9</sup> The best fit parameters obtained are listed in Table 6. Taking into account these results, our hypothesis ( $D = 0$ ) may be correct owing to the high  $J$  values and the  $R$  value obtained.

## Magnetostructural correlations

The Ni–N–N angle and the Ni–N<sub>azide</sub>–Ni torsion angle are the most significant structural parameters for monodimensional compounds with only one end-to-end azido bridge.<sup>4</sup> The maximum antiferromagnetic coupling is expected for Ni–N–N angles close to 108° and this coupling decreases at higher values with an accidental orthogonality valley centred at 165°. Taking into account the used hamiltonian  $H = -J \sum S_i S_{i+1}$ , the antiferromagnetic coupling is greater when the value of  $J$  is more negative. Furthermore, the best antiferromagnetic coupling appears when the torsion angles is 0° (or 180°) and diminishes when the torsion angles increases to

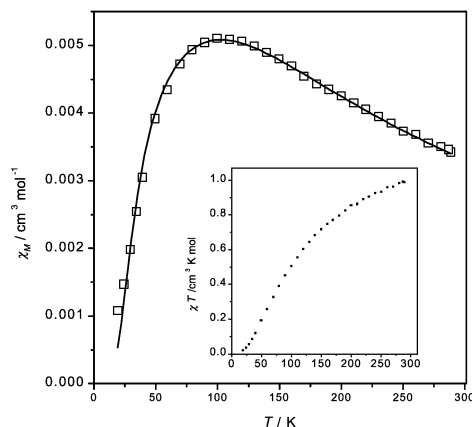


**Fig. 8** Plots of observed  $\chi_M$  and  $\chi_M T$  (inset) versus  $T$  for [Ni(*N*-Metn) $_2(\mu_{1,3}$ -N $_3$ )] $_2$ (ClO $_4$ ) $_2$  (**4**). Solid line represents the best theoretical fit (see text).

**Table 6** Best fitted magnetic parameters and structural parameters for (1), (2), (3) and (4)

Compound	$J/\text{cm}^{-1}$	$g$	$R$	Ni–N–N/ $^\circ$	Ni–(N <sub>3</sub> )–Ni torsion angle/ $^\circ$
(1)	–21.8	2.27	$1.04 \times 10^{-4}$	136.4, 149.8	161.2
(2)	–3.2	2.30	$4.45 \times 10^{-3}$	151.4	180.0
(3)	–42.3	2.34	$8.1 \times 10^{-5}$	136.5, 145.4	177.6
(4)	–69.6	2.27	$1.5 \times 10^{-4}$		

$R = \sum(\chi_M^{\text{calc}} - \chi_M^{\text{obs}})^2 / \sum(\chi_M^{\text{obs}})^2$ .

90°. For compounds (1) and (3), the Ni–N–N angles and the Ni–N<sub>azide</sub> distances are very similar whereas the Ni–N<sub>azide</sub>–Ni torsion angle is more different than 180° for compound (1) than for compound (3). This difference explains why the coupling is less antiferromagnetic in (1) than in (3) (see Table 6). On the other hand, compound (2) shows the optimum value for the Ni–N<sub>azide</sub>–Ni torsion angle (180°), but its Ni–N–N angles are 151.4°, greater than those of compound (1) and (3) and close to 165° at which the antiferromagnetic coupling is less favoured. Taking into account that the bond angle is the main structural factor in the superexchange pathway, a low  $J$  value would be expected for compound (2) which is consistent with experimental data.

For dinuclear compounds, superexchange coupling,  $J$ , between nickel centres through double  $\mu_{1,3}$ -N<sub>3</sub> bridges shows a wide range, between –114.5 and –4.6 cm<sup>–1</sup>.<sup>1</sup> In a previous study,<sup>10</sup> we demonstrated that  $J$  correlates strongly with the dihedral angle  $\delta$  (as defined above). We can see that there is a large decrease in  $J$  upon passing from dihedral angle 0° (maximum value) to 60° ( $J \cong 0$ ); whereas the distances Ni–N<sub>azide</sub> and other angles are less important. In the current case,  $\delta$  is 24.8°, and  $J = -70.0 \text{ cm}^{-1}$ . Consequently, this complex (4) is a new one which can be added with perfect agreement to the series previously reported for similar complexes.<sup>1</sup>

## Conclusions

We present the synthesis, single crystal structure and magnetostructural correlations of four novel compounds using

bidentate amines as ancillary ligand and azido bridges. Compounds (1), (2) and (3) are one-dimensional Ni<sup>II</sup> compounds with a single EE azido bridge and compound (4) is a dinuclear compound. All compounds show antiferromagnetic coupling and the values compare well with similar compounds reported in the literature and with the theoretical previsions.

## Acknowledgements

This work was undertaken with the financial support of CICYT BQU2000/0791. I. R. thanks Ministerio de Educación y Cultura for a doctoral FPI fellowship. We are very grateful to Dr. Nuria Clos for technical assistance with magnetic measurements.

## References

- 1 J. Ribas, A. Escuer, M. Monfort, R. Vicente, R. Cortés, L. Lezama and T. Rojo, *Coord. Chem. Rev.*, 1999, **193–195**, 1027.
- 2 C. S. Hong, J.-e. Koo, S.-K. Soon, Y. S. Lee, Y.-S. Kim and Y. Do, *Chem. Eur. J.*, 2001, **7**, 4243.
- 3 P. S. Mukherjee, S. Dalai, E. Zangrado, F. Lloret and N. R. Chaudhury, *Chem. Commun.*, 2001, 1444.
- 4 A. Escuer, R. Vicente, J. Ribas, M.-S. El Fallah, X. Solans and M. Font-Bardia, *Inorg. Chem.*, 1994, **33**, 1842.
- 5 (a) G.-M. Sheldrick, SHELXL-93, Program for the Solution for Crystal Structure, Universität Göttingen, Germany, 1993; (b) G.-M. Sheldrick, SHELXL-97, Program for the Solution for Crystal Structure, Universität Göttingen, Germany, 1997.
- 6 G.-M. Sheldrick, SHELXL-97, Program for the refinement of Crystal Structure, Universität Göttingen, Germany, 1997.
- 7 C.-Y. Weng, Ph.D. Thesis, Carnegie Institute of Technology, 1968.
- 8 (a) F. D. M. Haldane, *Phys. Rev. Lett.*, 1983, **50**, 1153; (b) F. D. M. Haldane, *Phys. Lett.*, 1983, **93A**, 464; (c) J. P. Renard, M. Verdager, L. P. Regnault, W. A. C. Erkelens, J. Rossat-Mignon and W. G. Stirling, *Europhys. Lett.*, 1987, **3**, 945; (d) J. P. Renard, M. Verdager, L. P. Regnault, W. A. C. Erkelens, J. Rossat-Mignon, J. Ribas, W. J. Stirling and C. J. Vettier, *Appl. Phys.*, 1988, **63**, 3538.
- 9 C. O'Connor, *J. Prog. Inorg. Chem.*, 1982, **29**, 239.
- 10 J. Ribas, M. Monfort, C. Diaz, C. Bastos and X. Solans, *Inorg. Chem.*, 1993, **32**, 3557.